Coexistence of oscillation and quenching states: Effect of low-pass active filtering in coupled oscillators

Cite as: Chaos **29**, 073110 (2019); https://doi.org/10.1063/1.5093919
Submitted: 21 February 2019 . Accepted: 21 June 2019 . Published Online: 19 July 2019

Xiaoqi Lei, Weiqing Liu, Wei Zou, and Jürgen Kurths

Coexistence of oscillation and quenching states: Effect of low-pass active filtering in coupled oscillators

Cite as: Chaos **29**, 073110 (2019); doi: 10.1063/1.5093919
Submitted: 21 February 2019 · Accepted: 21 June 2019 ·
Published Online: 19 July 2019

Xiaoqi Lei,[1] Weiqing Liu,[1,a)] Wei Zou,[2] and Jürgen Kurths[3,4,5]

AFFILIATIONS

[1]School of Science, Jiangxi University of Science and Technology, Ganzhou341000, China
[2]School of Mathematical Sciences, South China Normal University, Guangzhou510631, People's Republic of China
[3]Potsdam Institute for Climate Impact Research, Telegraphenberg, D-14415 Potsdam, Germany
[4]Institute of Physics, Humboldt University Berlin, BerlinD-12489, Germany
[5]Saratov State University, Saratov, Russia

Note: This paper is part of the Focus Issue on Symmetry and Optimization in the Synchronization and Collective Behavior of Complex Systems.
[a)]**Electronic mail:** wqliujx@gmail.com

ABSTRACT

Effects of a low-pass active filter (LPAF) on the transition processes from oscillation quenching to asymmetrical oscillation are explored for diffusively coupled oscillators. The low-pass filter part and the active part of LPAF exhibit different effects on the dynamics of these coupled oscillators. With the amplifying active part only, LPAF keeps the coupled oscillators staying in a nontrivial amplitude death (NTAD) and oscillation state. However, the additional filter is beneficial to induce a transition from a symmetrical oscillation death to an asymmetrical oscillation death and then to an asymmetrical oscillation state which is oscillating with different amplitudes for two oscillators. Asymmetrical oscillation state is coexisting with a synchronous oscillation state for properly presented parameters. With the attenuating active part only, LPAF keeps the coupled oscillators in rich oscillation quenching states such as amplitude death (AD), symmetrical oscillation death (OD), and NTAD. The additional filter tends to enlarge the AD domains but to shrink the symmetrical OD domains by increasing the areas of the coexistence of the oscillation state and the symmetrical OD state. The stronger filter effects enlarge the basin of the symmetrical OD state which is coexisting with the synchronous oscillation state. Moreover, the effects of the filter are general in globally coupled oscillators. Our results are important for understanding and controlling the multistability of coupled systems.

Oscillation states and oscillation quenching of coupled oscillators always compete with each other. These are vital regimes of many cooperative phenomena emerging in nature, especially in biological functions since oscillation suppression is significantly relevant in pathological cases of neuronal disorders such as Alzheimer's and Parkinson's disease. Due to various forms of coupling interaction, coupled oscillators may exhibit rich transition processes from oscillation states to several kinds of oscillation quenching, such as amplitude death (AD), symmetrical oscillation death, asymmetrical oscillation death, and nontrivial amplitude death (NTAD). Generally, frequency mismatches and different time scales are deemed to be two key factors that cause oscillation quenching. Low-pass filter (LPF), a general component in a circuit, has been verified to be beneficial to realize oscillation quenching in coupled oscillators owing to its characteristics of decaying signals whose frequency is larger than the cutoff frequency. Here, we report that a kind of low-pass active filter (LPAF), which is containing a LPF followed by an active component of amplifiers (or attenuators), significantly influences the dynamics of diffusively coupled as well as globally coupled oscillators. The parameter of cutoff frequency controls the dynamical regimes of the coupled oscillators, such as the coexistence of the oscillation states and several quenching regimes. Meanwhile, the competition between the filtering and the amplifying (or attenuating) effects of the active component of LPAF determines the fate of the coexistence of the symmetrical OD and NTAD. Our study opens new

ways of controlling the dynamical activity of complex nonlinear systems.

I. INTRODUCTION

Collective dynamics in coupled oscillators have been an attractive topic of extensive research in the field of physics, biology, and engineering owing to the fact that various coupled nonlinear oscillators provide a simple but efficient mathematical model to both qualitatively and quantitatively describe dynamical activities emerging in nature and engineering. Rich kinds of synchronization[1,2] and oscillation quenching,[3,4] which are related to regimes of pattern formation and self-organization behavior, have been observed in neurons, cardiac pacemakers,[2] and chemical experiments. Generally, there are two typical kinds of oscillation quenching, amplitude death (AD) and oscillation death (OD), where the former one is realized by stabilizing the original fixed points, thus leading to a stable homogeneous steady state (HSS) which is a state that two coupled oscillators are quenched to the same branch of fixed points, while the latter one occurs due to a stabilization of a newborn coupling-dependent inhomogeneous steady state (IHSS) which is a state that two coupled oscillators stay on two different fixed points. The dynamics of AD in coupled systems is widely explored in the field of engineering control such as suppressing undesirable oscillations in laser applications,[6–8] neuronal systems,[9] and electronic circuits.[10] Moreover, AD can be realized by various regimes such as parameter mismatches,[11] time scale diversity,[12] time-delay,[13–16] dynamical coupling,[17] conjugate variable coupling,[18] mean-field diffusion,[10,19–21] and indirect coupling.[22–24] In contrast, OD is much more significant for life science, since it relates to the essential mechanism of cellular differentiation,[25–27] synthetic genes,[28–30] and neurological conditions.[31,32] Moreover, OD can be widely observed in coupled oscillators with cyclic coupling,[33] repulsive coupling,[34,61] amplitude-dependent coupling,[35] or environmental coupling.[36] Both AD and OD are also common dynamics in regular networks (such as locally coupled[37,38] or all-to-all[39] coupled networks) and complex networks (such as small-world networks[40] or Scale-free networks[41,42]).

The transition scenarios between these two very distinct dynamical regimes, i.e., AD and OD, have become one of the most challenging open problems. Koseska *et al.*[4] observed a transition from AD to OD via a supercritical pitchfork bifurcation (PB) in a coupled nonidentical oscillator with an interplay between the heterogeneity and the coupling parameter that is analogous to the Turing-type bifurcation in spatially extended systems. Zou *et al.*[16] extended and enhanced the effect of AD-OD transition by including a time-delay so that the AD-OD transition can be induced even in identical Stuart-Landau oscillators. Further AD-OD transitions were reported in coupled oscillators with conjugate coupling,[43] cyclic coupling,[33] mean-field coupling,[20,21] and even symmetry-breaking repulsive coupling.[34,44] The inner regimes of AD-OD transition processes are important from the perspective of engineering control so as to determine the final fate of coupled oscillators. Meanwhile, coupled oscillators always exhibit the characteristics of multistable states in the transition processes which arise in many biological processes, such as bistability in brain activity[45] (e.g., sleep-wake cycle of mammals and birds), in the lac operon which is an operon required for the transport and metabolism of lactose in *Escherichia coli* and many other enteric bacteria,[46] in the cell cycle,[47] etc. For example, the evoking of multiple coexisting stable attractors with different features is observed in synthetic genetic networks with repressive cell-to-cell communication,[28] where the oscillating state is coexisting with the transition from an inhomogeneous steady state to an inhomogeneous limit cycle. Moreover, another novel oscillation quenching state, namely, a nontrivial AD (NTAD) state, is observed coexisting with OD which is realized by a subcritical pitchfork bifurcation in mean-field conjugate coupled oscillators.[43] Since the NTAD state is unique and sensitive to parameter mismatches, it is difficult to realize in coupled nonidentical oscillators, where AD may occur and be born via a subcritical pitchfork bifurcation with the aid of mean-field diffusive coupling[48] or conjugate coupling[43] in coupled identical oscillators. Compared to a general AD state, this NTAD state has not only a nonzero homogeneous steady state but, more significantly, in this state, the two coupled oscillators stand on the same positive (or negative) branch of fixed points and become bistable. Therefore, exploring the dynamics of the coexistence of NTAD and OD (or oscillation) is of great importance owing to the fact that it gives evidence of a direct transition from monostability (AD) to bistability (NTAD) in a dynamical system that may improve our understanding of the origin of bistability arising in biological processes.[45,46] The coexistence of OD and NTAD was first observed in conjugate coupled oscillators,[16] and then NTAD was reported coexisting with a limit cycle (or OD) in the presence of environmental coupling.[49]

In practical coupled systems, especially electrical and biological networks, the interacting terms may change the phase and the amplitude of the input signal which are similar to the characteristic of filter circuits. The low-pass filter (LPF) is omnipresent in the musculoskeletal system of the human body,[50] the abdominal ganglion of the crayfish,[51] and the block of phase-locked loops[20] and is widely applied in communication and chaos control.[52,53] In particular, the entrainment behaviors of relaxation oscillators coupled by LPFs have been investigated by conducting a series of experiments.[54] Moreover, LPFs have been found helpful to revoke AD and OD in coupled oscillators[55] as well as to significantly influence the stability of synchronization.[56,57] Meanwhile, LPF can lead to a symmetry-breaking transition from homogeneous to inhomogeneous limit cycles,[58] when it is applied in the self-feedback term of the coupling in a mean-field coupled system. The cutoff frequency of LPF is a key factor for determining the final fate of the coupled system. The coexistence of OD and an oscillating state can be observed in a small interval of parameters for a properly selected cutoff frequency. In this consideration, it is interesting to raise the question of how a LPF may influence the coexistence of oscillating states and the oscillation quenching states including AD, OD, and NTAD, and their transition processes. Does the attenuation effect of the filter play the key role on the dynamics of the coupled oscillators?

In this paper, we explore the dynamics of diffusively coupled identical paradigmatic oscillators with a low-pass active filter (LPAF). LPAF,[59] which consists of a LPF and an active component (amplifier or attenuator), may result in both dispersion and amplification (or attenuation) of the input signals. The LPF part of the LPAF passes low frequency signals (less than a cutoff frequency α) but attenuates high frequency signals (larger than a cutoff frequency α), as well as introduces certain phase shift. The additional active component of

LPAF (amplifier or attenuator) may adjust the amplitude of the output signals from LPF. The filtering effect of LPF is stronger as α is smaller since the input signals of LPF may be attenuated more as α is smaller. The competition between the filtering effects of LPF and the amplification (or attenuation) effects of the active component is expected to influence the transition processes of the coupled oscillators. In this way, a new transition process from AD to symmetrical OD, asymmetrical OD, asymmetrical oscillation which is coexisting with a synchronous large oscillation, is observed. Asymmetrical OD and asymmetrical oscillation state are two new kinds of dynamics regimes with which the symmetries between the two coupled oscillators are broken so that the two coupled oscillators stand on two different branches as $x_1(t)$ and $x_2(t)$ with $|x_1(t)| \neq |x_2(t)|$. As a comparison, the symmetrical OD is the ordinary OD state where the two coupled oscillators stand on two different branches as x_1^* and x_2^* with $x_1^* = -x_2^*$, where the time behavior of the two coupled systems is symmetrical to each other.

II. MODEL

The coupled Stuart-Landau oscillator is a general model to explore oscillation quenching.[3] Amplitude death can be observed in two coupled nonidentical Stuart-Landau oscillators with single-variable coupling[4] or dual-variable coupling.[5] Since we mainly focus on the effects of LPAF on the oscillation quenching dynamics of the coupled system, it is necessary to omit the effects of the frequency mismatches between two coupled oscillators. However, there is no AD or OD in the diffusively coupled identical oscillators unless repulsive coupling,[61] time-delay,[14] or dissimilar variable[18] is introduced. Based on the fact that there are rich dynamics, such as AD, OD, and AD-OD transitions, in the single-variable coupled identical oscillators,[4] we will consider this model to explore the effects of the LPAF on oscillation quenching. The model of the single-variable coupled two identical Stuart-Landau oscillators with an additional coupling media of LPAF is presented in the diagrammatic sketch in Fig. 1(a), which is modeled as a dynamical system in Eq. (1),

$$\begin{aligned}
\dot{Z}_1(t) &= [1 + j\omega - |Z_1(t)|^2]Z_1(t) + \epsilon(QS_2 - \mathrm{Re}(Z_1)),\\
\dot{S}_1(t) &= \alpha(-S_1 + \mathrm{Re}(Z_1)),\\
\dot{Z}_2(t) &= [1 + j\omega - |Z_2(t)|^2]Z_2(t) + \epsilon(QS_1 - \mathrm{Re}(Z_2)),\\
\dot{S}_2(t) &= \alpha(-S_2 + \mathrm{Re}(Z_2)),
\end{aligned} \tag{1}$$

where $\mathrm{Re}(Z_i)$ is the real part of the coupled system with complex variables $Z_i = x_i + jy, i = 1, 2$ with $j = \sqrt{-1}$. The individual Stuart-Landau oscillators have unit amplitude and eigenfrequency ω. ϵ represents the coupling strength, S_i represents the output signals of the LPF with the real input signals $\mathrm{Re}(Z_i)$, QS_i is the output signal of the active component in LPAF, where Q controls the degree of the amplification (or attenuation) to the output signals from the LPF. The active component following the LPF is an amplifier (or attenuator) as $Q(\in (1, 2])$ (or $Q \in [0, 1)$). Accordingly, the feedback signals are amplified (or attenuated) as $1 < Q \leq 2$ (or $0 \leq Q < 1$). The fixed points of Eq. (1) are presented in the form of $F(R^m, \sigma R^m)$ with $R^m = (x^m, y^m, x^m)$ and can be classified into three types as the trivial fixed point O for $R^m = (0, 0, 0)$, a pair of coupling-dependent inhomogeneous steady state F_{IHSS} for $m = *, \sigma = -1$, and a pair

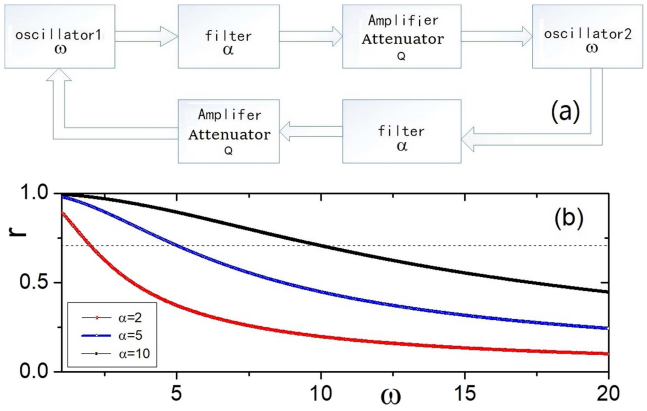

FIG. 1. (a) The schematic diagram of the diffusively coupled oscillators with LPAF where the amplifier (or attenuator) is the active component attached to LPF. (b) The amplitude-frequency response of the LPF with $\alpha = 2, 5, 10$, respectively.

of nontrivial homogeneous steady state F_{NHSS} for $m = +, \sigma = 1$, respectively, where x^*, y^*, and x^+, y^+ are presented in Eqs. (2) and (3),

$$\begin{aligned}
x^* &= -\frac{\omega y^*}{\epsilon(1+Q)y^{*2} + \omega^2},\\
y^* &= \pm\sqrt{\frac{\epsilon(1+Q) - 2\omega^2 + \sqrt{\epsilon^2(1+Q)^2 - 4\omega^2}}{2\epsilon(1+Q)}},
\end{aligned} \tag{2}$$

$$\begin{aligned}
x^+ &= -\frac{\omega y^+}{\epsilon(1-Q)y^{+2} + \omega^2},\\
y^+ &= \pm\sqrt{\frac{\epsilon(1-Q) - 2\omega^2 + \sqrt{\epsilon^2(1-Q)^2 - 4\omega^2}}{2\epsilon(1-Q)}}.
\end{aligned} \tag{3}$$

Note that the existence of the nontrivial homogeneous steady state (NHSS) and inhomogeneous steady state (IHSS) is related to the coupling strength and the attenuation (or amplification) coefficient Q. The NHSS and IHSS may disappear for some parameters of ϵ and Q (e.g., NHSS disappears for $Q = 1$), while the original trivial fixed points O keep for all parameters. The parameter α is the cutoff frequency of LPF. LPF passes signals with a frequency lower than α and attenuates signals with frequencies higher than α. Figure 1(b) represents the amplitude-frequency response curves for $\alpha = 2, 5, 10$, respectively, where the variable r is the amplitude of the output signal from LPF and variable ω is the natural frequency of the input signals of LPF (here, the input signals are from a single Stuart-Landau oscillator with parameter $\omega \in [0, 20]$). Obviously, the amplitude of the output signals of LPF may be attenuated to less than $\sqrt{2}/2$ times of its input signals as ω is larger than the cutoff frequency α. Smaller α means stronger filtering effects. If no LPF but only the active component is applied, then $\alpha \to \infty$. In this case, the dynamics equation of Eq. (1) degenerates to Eq. (4),

$$\begin{aligned}
\dot{Z}_1(t) &= [1 + j\omega - |Z_1(t)|^2]Z_1(t) + \epsilon(QRe(Z_2) - Re(Z_1)),\\
\dot{Z}_2(t) &= [1 + j\omega - |Z_2(t)|^2]Z_2(t) + \epsilon(QRe(Z_1) - Re(Z_2)).
\end{aligned} \tag{4}$$

The fixed points of the coupled oscillators without filter then become four arguments, $O(0,0,0,0)$, $F_{IHSS}(x^*, y^*, -x^*, -y^*)$, $F_{NHSS}(x^+, y^+, x^+, y^+)$. Note that the cutoff frequency α has no effects on the existence of the fixed points but influences the stability of the fixed points. As a comparison, Q influences both the existence of the fixed points and their stabilities.

III. DYNAMICS OF COUPLED OSCILLATORS WITHOUT LPF

Let us first consider the dynamics of the coupled oscillators without filters as presented in Eq. (4) [$\alpha = \infty$ and $S_i = \mathrm{Re}(Z_i)$, $i = 1, 2$ in Eq. (1)]. The final regime of the coupled system is determined by the existence of the fixed points and their stabilities. In particular, the existence of IHSS is determined by whether y^* is real which leads to Eq. (5). The boundary lines in yellow and red are presented in Fig. 2(a) for the coupled oscillators with an attenuator ($Q = 0.8$) and in Fig. 2(c) for the coupled oscillators with amplifier ($Q = 1.2$), respectively,

$$\begin{aligned} \frac{1}{1+Q} < \epsilon < \frac{1+\omega^2}{1+Q}, \\ \frac{2\omega}{1+Q} < \epsilon \le \frac{1}{1+Q}. \end{aligned} \tag{5}$$

Meanwhile, F_{NHSS} exists only when y^+ is real which leads to Eq. (6) [cyan and magenta lines in Fig. 2(a) for $Q = 0.8$] and Eq. (7) [blue line in Fig. 2(c) for $Q = 1.2$],

$$\epsilon > \frac{1+\omega^2}{1-Q}, \quad \epsilon > \frac{2}{1-Q}, \quad 0 < Q < 1, \tag{6}$$

$$\frac{2\omega}{1-Q} < \epsilon \le \frac{2}{1-Q}, \quad 0 < Q < 1,$$

$$\epsilon > \frac{2\omega}{Q-1}, \quad 1 < Q \le 2. \tag{7}$$

The stability of all these fixed points is completely determined by the eigenvalues of the Jacobian matrix. The maximal real parts of the eigenvalues of the existing real IHSS and NHSS are all negative for all parameter ϵ and ω as $Q \in (0, 1)$. Therefore, the domains of IHSS and NHSS are determined by their existence as $Q \in (0, 1)$. Equation (8) presents the eigenvalues of the Jacobian matrix on the original fixed points $O(0,0,0,0)$,

$$\lambda_{1,2,3,4} = 1 - \frac{\epsilon(1 \pm Q)}{2} \pm \frac{\sqrt{(\epsilon(1+Q))^2 - 4\omega^2}}{2}. \tag{8}$$

As $Q \ge 1$, $\mathrm{Re}(\lambda_{1,2,3,4}) > 0$, the original fixed points never become stable for all ϵ and ω. As $0 < Q < 1$, the boundary lines of the AD state can be predicted by the negative maximal real part of the eigenvalue as presented in Eq. (9) [yellow lines in Fig. 2(a) for $Q = 0.8$],

$$\frac{2}{1-Q} < \epsilon < \frac{1+\omega^2}{1+Q}. \tag{9}$$

Due to the effects of the attenuator ($0 < Q < 1$), our numerical results show that there are 5 domains [AD (white area I), oscillation

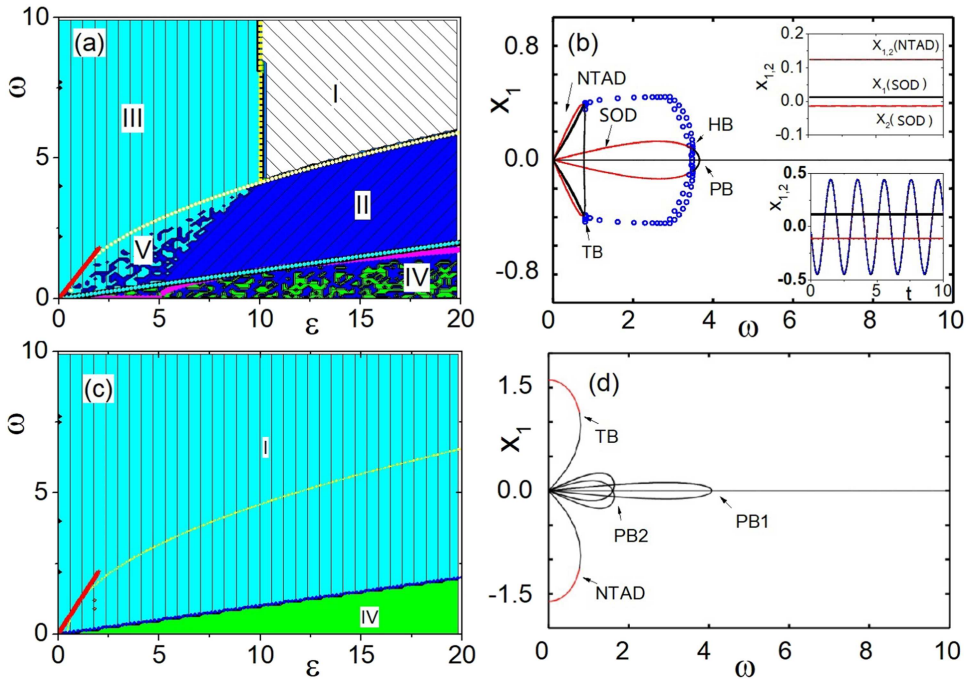

FIG. 2. (a) The phase diagram ω vs ϵ of the damply ($Q = 0.8$) coupled system without low-pass filter $\alpha = \infty$. There are five regimes as AD (area I), oscillation state (area II), SOD (area III), coexistence of NTAD and SOD (area IV), and coexistence of oscillation state and SOD (area V). (b) Bifurcation diagram (using XPPAUT) of two coupled identical Stuart-Landau oscillators for $\epsilon = 8.0$ and $Q = 0.8$: red lines, stable fixed points, black lines, unstable fixed points, blue circles, unstable limit cycles. The upper (lower) inset is the time series of $x_{1,2}$ for $\omega = 0.5(3.2)$ for $\epsilon = 8.0$, $Q = 0.8$, where NTAD($x_1 = x_2$) is coexisting with SOD ($x_1 = -x_2$), and SOD is coexisting with the oscillating state. (c) The phase diagram ω vs ϵ with the amplifier ($Q = 1.2$) in the coupled oscillators. There are two regimes as OS (area II) and NTAD (area IV). (d) Bifurcation diagram (using XPPAUT) of two coupled identical Stuart-Landau oscillators for $\epsilon = 8$ and $Q = 1.2$.

state (cyan area II), OD (blue area III), coexistence of NTAD and OD (mixed green and blue in area IV), coexistence of OD and oscillation state (mixed cyan and blue area V)] in the $\omega \sim \epsilon$ parameter space for the given $Q = 0.8$ as presented in Fig. 2(a). The numerical results coincide well with the theoretical predictions. Since the numerical results are presented for one set of initial conditions, there are two mixed colors green and blue in the coexisting area of AD and OD. Figure 2(b) shows the bifurcation diagram of x_1 (using XPPAUT) for $Q = 0.8$, $\epsilon = 8$. It is observed that an inverse pitchfork bifurcation (PB) occurs and the unstable original fixed point O transits to two unstable IHSS states at $\omega_{PB} = 3.661$ which is the right boundary line in Eq. (5) ($\epsilon < \frac{1+\omega^2}{1+Q}$), i.e., $\omega_{PB} = \sqrt{\epsilon(1+Q)-1}$ ($\omega_{PB} = 3.661$ for $Q = 0.8$ and $\epsilon = 8$). Both of the unstable IHSS transit to stable IHSS after a Hopf bifurcation (HB). Oscillation death is coexisting with the oscillation state in the interval of $\omega \in [0.7676, 3.486]$ for $Q = 0.8$ and $\epsilon = 8$. The coexistence of OD and oscillating state is verified by the time series of $x_{1,2}$ in the lower inset of Fig. 2(b) at $\omega = 3.2$. Note that a new kind of NTAD state emergences by stabilizing the NHSS via a tangential bifurcation (TB) at $\omega_{TB} = 0.8$ which is the left boundary line in Eq. (6) ($\epsilon > \frac{2\omega}{1-Q}$), i.e., $\omega_{TB} = \frac{\epsilon(1-Q)}{2}$ ($\omega_{TB} = 0.8$ for $\epsilon = 8$ and $Q = 0.8$). The attribute nontrivial to this AD state comes from the fact that it emerges from the nontrivial HSSs (x^+, y^+), which are nonzero and subsequently distributed symmetrically around zero. It has two different solutions $x_1 = x_2 = x^+$ and $x_1 = x_2 = -x^+$. The occurrence of one of these two states is determined by the initial conditions which has a striking resemblance to bistability. Moreover, since the former IHSS remains stable for $\omega < \omega_{TB}$, OD coexists with the NTAD for $\omega < \omega_{TB}$ which is confirmed by the time series of $x_{1,2}$ at two sets of initial conditions for $\epsilon = 8$, $\omega = 0.5$, and $Q = 0.8$ [upper insets of Fig. 2(b)]. The coexistence of OD and NTAD was found earlier by a supercritical pitchfork bifurcation in conjugate coupled oscillators[16] or by subcritical pitchfork bifurcation in mean-field diffusively coupled oscillators.[48] The genesis of NTAD and the origin of coexistence in our results are different from those mentioned above. The TB is responsible for the birth of the NTAD state. Further, the TB happened in the parameter of the oscillator unit other than the coupling strength. As we consider the effects of the amplifier on the dynamics of the coupled oscillators without filter, there are two domains [OS (cyan area II) and NTAD (green area IV)] in the parameter space ω vs ϵ for the given $Q = 1.2$ as presented in Fig. 2(c). The bifurcation diagram in Fig. 2(d) shows that the coupled oscillators transit from the unstable HSS to the symmetrical unstable IHSS via an inverse pitchfork bifurcation (PB1), and then transit to asymmetrical unstable IHSS via an inverse pitchfork bifurcation (PB2), and finally becoming NTAD via a TB. The attribute symmetry of IHSS derives from $x_1^* = -x_2^*$, where the two coupled oscillators stay symmetrically to the x axis. The symmetry is broken after PB2 and then leads to $x_1^* \neq -x_2^*$. Without the symmetrical attribution, the analytical solution of the asymmetrical IHSS cannot be figured out. Note that the HSSs and IHSSs are all unstable for $Q \in (1, 2]$ without LPF.

IV. EFFECTS OF LPAF

As a LPAF is applied to coupled oscillators, the parameter α of the LPF may influence the stabilities of HSS, IHSS, and NTAD. The onset conditions for AD and OD are determined by the characteristic eigenvalue equations obtained from the standard linear stability analysis of the coupled oscillators at its HSS and IHSS, respectively. A limit cycle occurs via a Hopf bifurcation. The Jacobian matrix of the system at the fixed points $F(R^m, \sigma R^m)$ of the coupled oscillators Eq. (1) is

$$J = \begin{pmatrix} C_{11} & C_{12} & 0 & 0 & D_{11} & 0 \\ C_{21} & C_{22} & 0 & 0 & 0 & 0 \\ 0 & 0 & \alpha & 0 & -\alpha & 0 \\ 0 & 0 & C_{11} & C_{12} & 0 & D_{11} \\ 0 & 0 & C_{21} & C_{22} & 0 & 0 \\ \alpha & 0 & 0 & 0 & 0 & -\alpha \end{pmatrix}, \tag{10}$$

where $C_{11} = (1 - 3(x^m)^2 - (y^m)^2 - \epsilon)$, $C_{12} = (-\omega - 2x^m y^m)$, $C_{21} = (\omega - 2x^m y^m)$, $C_{22} = (1 - (x^m)^2 - 3(y^m)^2)$, and $D_{11} = \epsilon Q$. Then, the characteristic equation of the system at the fixed point $F(A^m, \sigma A^m)$ can be expressed as

$$(\lambda^3 + P_2\lambda^2 + P_1\lambda + P_0)(\lambda^3 + P_2'\lambda^2 + P_1'\lambda + P_0') = 0, \tag{11}$$

where

$$\begin{aligned} P_2 &= -2 + 4(r^m)^2 + \epsilon + \alpha, \\ P_1 &= 1 + \alpha[4(r^m)^2 - 2 + \epsilon(1-Q)] + \omega^2 + 3(r^m)^4 - 4(r^m)^2 \\ &\quad - \epsilon(1 - (r^m)^2 - 2(y^m)^2), \\ P_0 &= \alpha[1 - 4(r^m)^2 + 3(r^m)^4 + \omega^2 - \epsilon(1-Q)(1 - (r^m)^2 - 2(y^m)^2)], \end{aligned} \tag{12}$$

$$\begin{aligned} P_2' &= -2 + 4(r^m)^2 + \epsilon + \alpha, \\ P_1' &= 1 + \alpha[4(r^m)^2 - 2 + \epsilon(1+Q)] + \omega^2 + 3(r^m)^4 - 4(r^m)^2 \\ &\quad - \epsilon(1 - r^m)^2 - 2(y^m)^2), \\ P_0' &= \alpha[1 - 4(r^m)^2 + 3(r^m)^4 + \omega^2 - \epsilon(1+Q)(1 - (r^m)^2 - 2(y^m)^2)], \end{aligned} \tag{13}$$

and $(r^m)^2 = (x^m)^2 + (y^m)^2$. The fixed points become stable if and only if the maximal real part of the eigenvalues is negative. Then, the role of the cutoff frequency α can be well understood by deriving the important bifurcation curves from the characteristic equation (11). Since Eq. (11) is a sixth-order polynomial and is difficult to extract bifurcation points from the eigenvalue analysis, we apply the technique in Ref. 60 to predict the HB points from the coefficients of the characteristic equation itself. The HB points of the AD states can be derived by putting $|P_1P_2 - P_0|_{(x^m=0, y^m=0)} = 0$,

$$\omega_{HB1} = \sqrt{\frac{(\alpha + \epsilon - 1)(2\alpha + \epsilon - 2 - \alpha\epsilon(1-Q))}{\epsilon - 2}}. \tag{14}$$

The HB points of IHSS can be determined by using $|P_1P_2 - P_0|_{F_{IHSS}} = 0$. It cannot be expressed as a function of ω_{HB2} but of α_{HB2},

$$\alpha_{HB2} = \frac{-B_{HB2} + \sqrt{B_{HB2}^2 - 4A_{HB2}C_{HB2}}}{2A_{HB2}}, \tag{15}$$

where $A_{HB2} = -2 + 4(r^*)^2 + \epsilon(1-Q)$, $B_{HB2} = (-2 + 4(r^*)^2 + \epsilon(1-Q))(-2 + 4(r^*)^2 + \epsilon) - \epsilon Q(1 - (r^*)^2 - 2(y^*)^2)$, $C_{HB2} = (-2 + 4(r^*)^2 + \epsilon)(1 + \omega^2 + 3(r^*)^4 - 4(r^*)^2 - \epsilon(1 - (r^*)^2 - 2(y^*)^2)$, *and* $(r^*)^2 = (x^*)^2 + (y^*)^2$.

A. Effects of LPF and attenuators

We examine the effects of the LPF in addition to the attenuating active component ($Q \in [0, 1)$) on the coupled dynamics in dependence on the cutoff frequency α. Figures 3(a)–3(c) present the phase diagram in the $\omega \sim \epsilon$ parameter space for $\alpha = 10, 3, 1$, respectively. Compared to that for $\alpha = \infty$ [Fig. 2(a)], the domains of AD increase but those of the coexistence of OD and NTAD (area IV with mixed green and blue colors) keep constant as α decreases from ∞ to 1. Note that the left boundary of the AD domain coincides with the Hopf bifurcation (HB1) critical line. However, the right boundary of the AD domain is higher than the Hopf bifurcation (HB1) lines [red dotted lines in Figs. 3(a)–3(c)]. Moreover, the OD domains shrink by increasing the domains of the coexistence of OD and OS states [area V with mixed blue and cyan enclosed by the yellow and purple lines in Figs. 3(a)–3(c)] for $\alpha = 10, 3, 1$. Since the colored areas are recorded numerical results with one set of initial conditions for each parameter, two colors are mixed in the coexisting area. The more dense one color is, the large the basin of the corresponding regime is. The effects of α on the dynamics are more clearly indicated by the possibility of AD, OD, and OS (defined as $P_{st} = \frac{S_{st}}{S_{tol}}$, where st is the state of AD, OD, or OS, S_{st} is the area of domain st, S_{tol} is the area of the domain of parameter space $\epsilon \in [0, 20]$ vs $\omega \in [0, 10]$) vs α shown in Fig. 3(d). P_{AD} increases linearly with the decrease of α, and P_{OD} decreases as α decreases from 20 to 1. P_{NTAD} keeps constant for all α.

To make the transition processes clearer, the bifurcation diagrams for ω are presented in Figs. 3(e) and 3(f) for $\epsilon = 8.0$ and $\alpha = 10, 1$, respectively. We find that the coupled oscillators transit from AD to the OS via Hopf bifurcation (HB1) at $\omega_{HB1} = 5.323$ [Eq. (14)] for $\alpha = 10$. An unstable IHSS occurs via a pitchfork bifurcation from the unstable HSS at $\omega = 3.661$ and then becomes stable IHSS (OD) at a reverse Hopf bifurcation (HB2) ($\omega_{HB2} = 3.486$). The limit cycle generated from HB1 coexists with the stable IHSS in the interval of $\omega \in [1.811, 3.486]$ and then disappears as $\omega \leq 1.811$. The coexistence of OD and NTAD keeps in the interval of $\omega \in (0, 0.8]$. As $\alpha = 1$, HB1 decreases to $\omega_{HB1} = 2.921$ and generates an unstable limit cycle which transits to a stable one at $\omega = 2.371$. Meanwhile, the former unstable HSS state becomes the stable HSS (AD) and transits to the stable IHSS (OD) via PB at $\omega_{PB} = 3.661$ as shown in Fig. 3(f). The coexistence of the stable limit cycle and the OD states occurs in the interval $\omega \in [0.7793, 2.371]$. Note that α influences the transition points of HB1 and the stability of HSS, IHSS, NTAD, and the limit cycle but has no obvious effects on the transition points of PB and TB. Let us consider the effects of α on the basin of the coexisting states. Figures 4(a) and 4(b) present the basins (in $x_{20} = y_{20}$ vs $x_{10} = y_{10}$) of two coexisting OD and NTAD for $\epsilon = 8$, $\omega = 0.5$, and $\alpha = 1, 10$, respectively. The increment of α slightly enlarges the basin of the two coexisting OD and NTAD as shown in the proportion of basins vs α in Fig. 4(c). According to the basins of the coexisting OD and OS state in Figs. 4(d) and 4(e) and the proportion of basins vs α in Fig. 4(f), the basins of OD enlarge as α increases from 1 to 20.

B. Effects of LPF and amplifier

Now, we consider both the effects of the filter and the amplifying active component ($Q > 1$) on the dynamics of the coupled oscillators. With the amplifier, the increment of α tends to shrink the area of both AD and SOD domains in the $\omega \sim \epsilon$ parameter space. The SOD domains are shrunk by increasing the domains of the coexisting SOD and OS. However, the area of the NTAD domain is slightly enlarged. As α is large, for example, $\alpha = 8$ [shown in Fig. 5(c)], the coupled oscillators transit from AD to OS via HB1 at

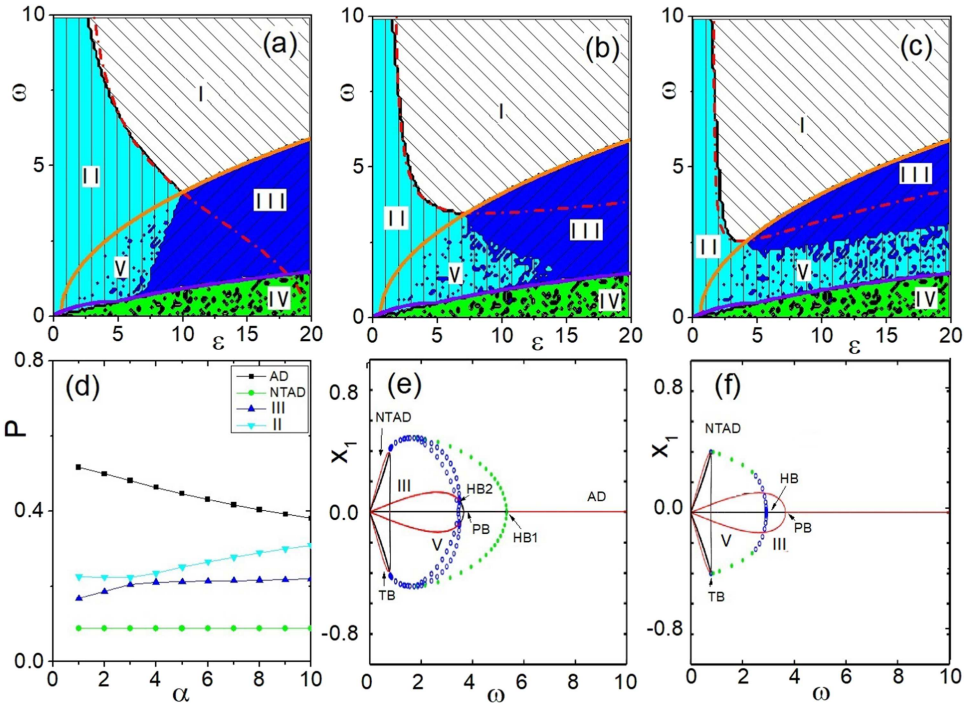

FIG. 3. (a)–(c) The phase diagram ω vs ϵ of the damply ($Q = 0.8$) coupled system with LPF for $\alpha = 10, 3, 1$, respectively. The red dashed lines are the critical lines of HB1 predicted in Eq. (14). There are five regimes as AD (area I), oscillation state (area II), SOD (area III), coexistence of NTAD and SOD (area IV), and coexistence of SOD and oscillation state (area V). (d) The proportions of AD (black squared dotted line), oscillation state (reversed triangle dotted line), SOD (triangle dotted line), and NTAD (circle dotted line) domains in the parameter spaces of ϵ and ω vs cutoff frequency α. (e) and (f) Bifurcation diagram of x_1 vs ω for the given $\epsilon = 8.0$ and $\alpha = 10, 1$, respectively.

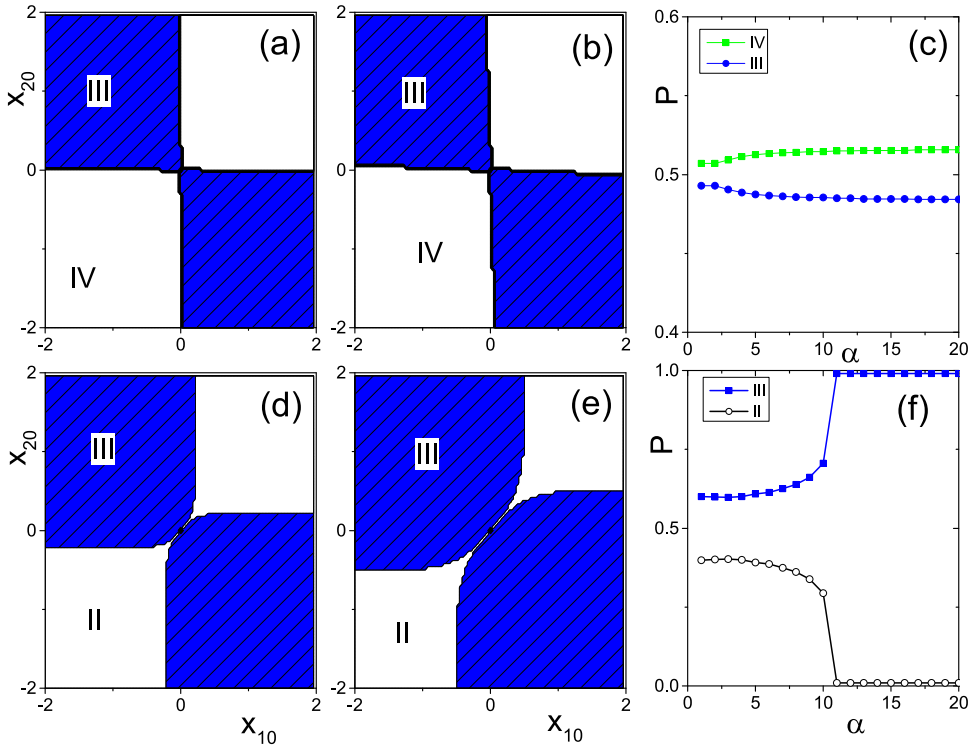

FIG. 4. (a) and (b) The basins of the coexisting SOD (blue, III) and NTAD (white, IV) in $x_{10} = y_{10}$ and $x_{20} = y_{20}$ for $\epsilon = 8, \omega = 0.5$, $Q = 0.8$, $\alpha = 1, 10$, respectively. (d) and (e) The basins of coexisting SOD (blue, III) and oscillation state (white, II) in $x_{10} = y_{10}$ and $x_{20} = y_{20}$ for $\epsilon = 8$, $\omega = 2.0$, $Q = 0.8$, $\alpha = 1, 10$, respectively. (c) and (f) The proportion of SOD (blue dotted lines) vs α for $\epsilon = 8$, $Q = 0.8$, $\omega = 0.5, 2.0$, respectively.

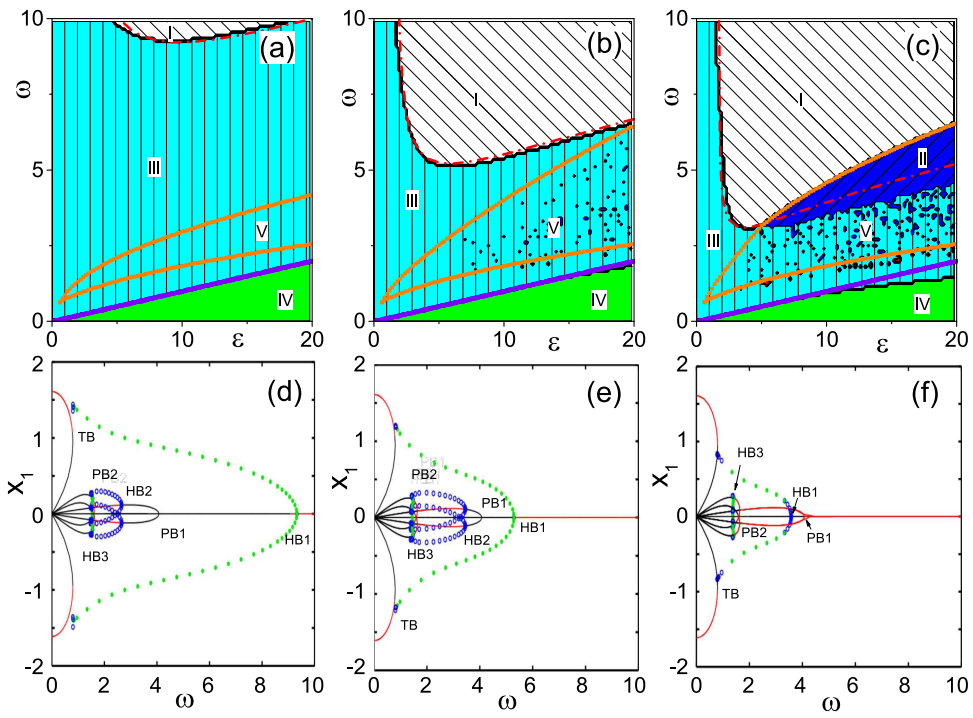

FIG. 5. (a)–(c) The phase diagrams ω vs ϵ of the coupled system with the amplifier ($Q = 1.2$) and the LPF for $\alpha = 8, 3, 1$, respectively. The red dashed lines are the critical lines of HB1 predicted in Eq. (14). There are seven domains as I (AD), II (symmetrical OD), III (oscillation state), IV (NTAD), V (coexistence of symmetrical OD and oscillation state enclosed by the orange critical lines), VI (coexistence of oscillation state and NTAD), and VII (coexistence of oscillation state and asymmetrical OD). (d)–(f) The bifurcation diagram of x_1 vs ω for the given $\epsilon = 8.0$ and $\alpha = 8, 3, 1$, respectively.

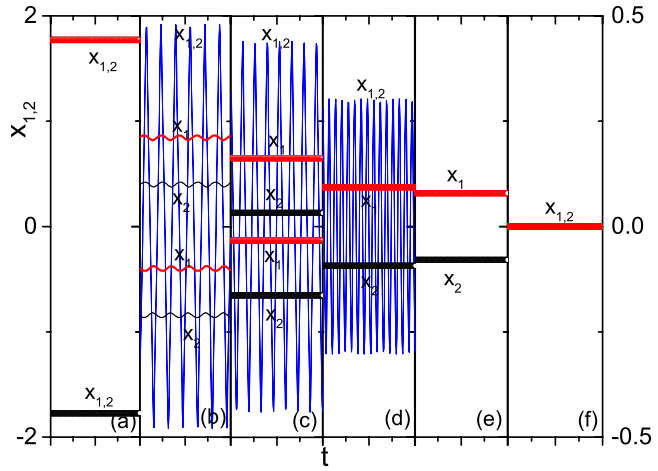

FIG. 6. The time series of $x_{1,2}$ for $\epsilon = 8.0, \alpha = 1, Q = 1.2$, and (a) $\omega = 0.5$ (b) $\omega = 1.39$, (c) $\omega = 1.5$, (d) $\omega = 3.0$, (e) $\omega = 3.8$, (f) $\omega = 6.0$.

$\omega_{HB1} = 9.327$ [Eq. (14)]; meanwhile, the stable HSS (AD) becomes the unstable HSS after HB1, and then the unstable HSS transits to an unstable IHSS via the supercritical pitchfork bifurcation (PB1) at $\omega_{PB1} = 4.074$. The unstable IHSS becomes the stable IHSS (SOD) after HB2 where a pair of unstable limit cycles is generated at $\omega_{HB2} = 2.658$. The stable IHSS (symmetrical OD) transits to the asymmetrical stable IHSS (asymmetrical OD) via supercritical PB2 at $\omega_{PB2} = 1.636$ and then to the oscillating state via HB3, where the asymmetrical stable IHSS becomes an unstable IHSS at $\omega_{HB3} = 1.548$. The oscillating limit cycle originated from HB1 (large oscillation) is coexisting with the transition processes from PB2 to HB3. As a result, the large oscillation state is first coexisting with the symmetrical OD, then coexisting with the asymmetrical OD, and finally coexisting with the small oscillation state [in area VII of Fig. 5(c)] as ω decreases from 3.5 to $\omega = 0.8$ where the stable NTAD occurs via a tangential bifurcation. The transition points of HB3, HB2, and HB1 become $\omega_{HBi} = 5.292, 3.453, 1.47$ $(i = 3, 2, 1)$ for $\alpha = 3$ and $\omega_{HBi} = 3.578, 3.578, 1.4$ $(i = 3, 2, 1)$ for $\alpha = 1$, respectively. The decrease of α tends to decrease the transition points of HB1 and HB3 and increase the transition point of HB2, however, keep the transition points of PB1 and PB2 constant. Therefore, the parameter interval of the stable IHSS coexisting with the limit cycle (area V) shrinks as the transition point HB2 approaches the transition point PB2 for decreasing α. Furthermore, the transition points HB1 and HB2 collide at $\omega = 3.578$ for $\alpha = 1$ and the unstable IHSS near PB1 becomes a stable IHSS. Therefore, α influences not only the stabilities of the fixed points but also the transition points of different states. Stronger filter effects (smaller α) tend to enhance the stability of both AD, symmetrical OD, and asymmetrical OD.

To confirm the transition processes in ω, we integrated the system equation with $\epsilon = 8$, $\alpha = 1$, and proper conditions (using the fourth-order Runge-Kutta method, with the step size equal to 0.005). Figure 6(a) shows the time traces for $\omega = 0.5$, where the NTAD states are observed. Figures 6(b)–6(d) present the coexistence of the limit cycle and the transitions from the symmetrical OD to the asymmetrical OD and then to the symmetrical oscillation state [the oscillating time series of two coupled oscillators are not symmetrical to each other $x_1(t) \neq -x_2(t)$ as shown in the red and black lines in Fig. 6(b)] for $\omega = 1.39, 1.5, 3.0$, respectively. In Fig. 6(b), we observe the two coexisting oscillating states, (1) two oscillators synchronously oscillate with a large amplitude $[x_1(t) = x_2(t)]$ and (2) two oscillators oscillate asymmetrically around different centers which can be two different positive or negative values. In Fig. 6(c), the asymmetrical oscillations transit to the asymmetrical IHSS which are positive or negative. In Fig. 6(d), the asymmetrical IHSS transits to the symmetrical IHSS. Figures 6(e) and 6(f) show the time traces of the symmetrical IHSS and AD for $\omega = 3.8, 6$, respectively, where the large synchronous oscillation disappears. Those time traces exhibit well the transition processes of the coupled oscillators.

Now, let us consider the effects of α on the basin of the coexisting oscillation state and the symmetrical IHSS. As an example, the basins of OS and IHSS are recorded by letting $x_{10} = y_{10}$ and $x_{20} = y_{20}$ for the parameters $\omega = 2, \epsilon = 8, Q = 1.2$, and $\alpha = 20, 1$ in Figs. 7(a) and 7(b), respectively. The basins of SOD for $\alpha = 20$ are smaller to those of SOD for $\alpha = 1$. The proportion of SOD (OS) basins increases (decreases) with the decrease of α as shown in Fig. 7(c). Therefore, the stronger filter effects tend to enlarge (shrink) the basin of SOD in LPF-coupled oscillators with an amplifier (attenuator).

To better understand the effects of the additional amplifier or attenuator on the coupled oscillators with strong filtering, we present the phase diagram of ϵ vs Q for the given $\epsilon = 8$, $\alpha = 1$, and $\omega = 1, 2, 3$, respectively, in Figs. 8(a)–8(c). The domains of NTAD

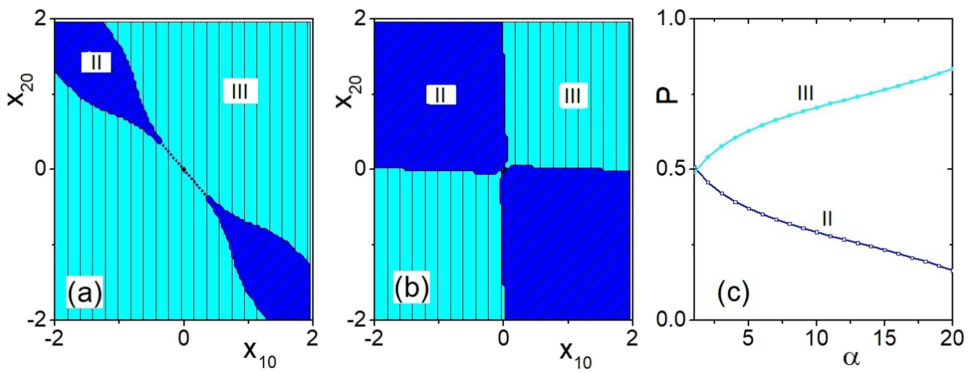

FIG. 7. The basins of the coexisting symmetrical OD (blue, area II) and oscillation state (cyan, area III) in $x_{10} = y_{10}$ and $x_{20} = y_{20}$ for $\epsilon = 8, \omega = 2$, $Q = 1.2$, and (a) $\alpha = 20$, (b) $\alpha = 1$. (c) The proportion of symmetrical OD (blue) and oscillation state (cyan) vs the parameter α.

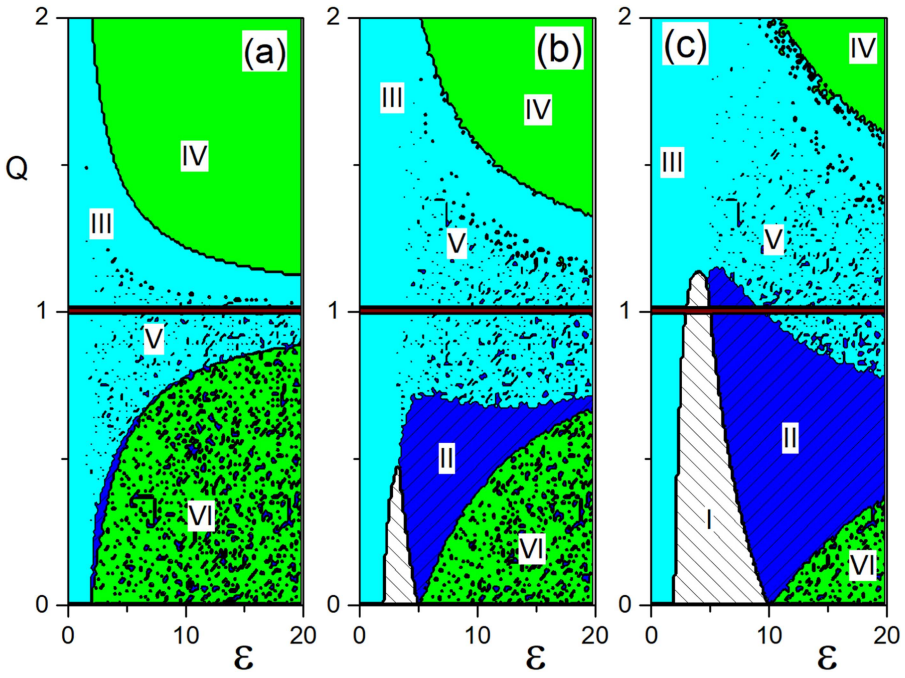

FIG. 8. The phase diagrams of Q vs ω for $\alpha = 1$ and (a) $\omega = 1$, (b) $\omega = 2$, (c) $\omega = 3$, respectively. There are six domains as I (AD), II (symmetrical OD), III (oscillation state), IV (NTAD), V (coexistence of symmetrical OD and oscillation state enclosed by the orange critical lines),VI (coexistence of oscillation state and NTAD).

are symmetrical to $Q = 1$; however, NTAD is coexisting with SOD as the attenuator is applied to a filter ($0 < Q < 1$); otherwise, NTAD is unique dynamics as an amplifier is applied to the filter ($1 < Q \leq 2$). Note that the domains of the coexisting SOD and NTAD decrease for the increase of the coefficient of the attenuator for $\omega = 1$. As a comparison, the domains of the NTAD are enlarged to the increase of the coefficient of the amplifier applied to the filter ($1 < Q \leq 2$) for $\omega = 1$. As the frequency of the oscillator is larger ($\omega = 2, 3$), AD domains occur and are enlarged as the coefficient of the attenuator Q ($Q < 1$) decreases. Both the domains of NTAD and those of the coexistence of SOD and OS shrink for the increase in the coefficient of amplifiers ($1 < Q \leq 2$).

C. The effects of LPAF in globally coupled oscillators

The effects of the LPAF on the oscillation quenching dynamics are not exclusive in the two coupled identical oscillators but also in multicoupled identical oscillators. For simplicity, the globally coupled Stuart-Landau oscillators are considered as

$$\begin{aligned} \dot{Z}_i(t) &= [1 + j\omega - |Z_1(t)|^2]Z_1(t) + \epsilon(QS_i - \mathrm{Re}Z_i)), \\ \dot{S}_i(t) &= \alpha\left(-S_i(t) + \frac{1}{N-1}\sum_{k=1,k\neq i}^{N}\mathrm{Re}(Z_i)\right), \quad i = 1, 2, \ldots, N. \end{aligned} \tag{16}$$

Without the LPAF, the coupled oscillator is the same as the mean-field coupling model discussed in Ref. 62 where two coupled oscillators may transit from complete synchronization to AD with the increment of the coupling strength for the given Q. Moreover, the left critical coupling strength of AD increases with the increments of the parameter $Q \in (0, 1)$. Now, let us extend the model to $N = 4$ and consider the effects of the LPAF. Equation (16) also has the trivial fixed point O and the NHSS $[F_{NHSS}(R^+, R^+, R^+, R^+)]$ and the symmetrical IHSS $F_{IHSS}(R^*, -R^*, R^*, -R^*)$, where x^+, y^+, of R^+ are the same as those in Eq. (3), and x^*, y^* in R^* have the same form as those in Eq. (2) but Q is replaced by Q' with $Q' = \frac{Q}{3}$. Therefore, the boundaries of the existence of F_{NHSS} are the same as those in Eqs. (6) and (7) and the boundaries of the existence of F_{IHSS} are determined by the equations with the same form as Eq. (5) whose Q is replaced by Q' with $Q' = \frac{Q}{3}$.

By integrating Eq. (16) with different parameters $\alpha = 8, 1$, the dynamical phase diagrams are presented in Figs. 9(a) and 9(b) for $Q = 0.8$ and in Figs. 9(c) and 9(d) for $Q = 1.2$, respectively. As $Q = 0.8$, there are six domains of different dynamics regimes as AD (area I), OD (area II), oscillation state (area III), coexistence of NTAD, symmetrical OD, and asymmetrical OD(area IV), coexistence of oscillation state and symmetrical OD (area V), coexistence of asymmetrical OD, symmetrical OD, and oscillation state (area VI). The bifurcation diagrams of x_1 vs ω for $\epsilon = 10$ [Figs. 9(a) and 9(b)] exhibit the transition processes clearly. As ω decreases from 6 to 0, the globally coupled oscillators transit from AD to OS via Hopf bifurcation, where the original fixed point O loses its stability and transits to SOD via pitchfork bifurcation (PB1). Note that three pairs of IHSS are born via pitchfork bifurcation (PB1) with one pair being stable and the other two pairs unstable. The unstable two pairs of IHSS become stable as they meet the new unstable symmetrical IHSS generated from another pitchfork bifurcation (PB2) which leads to the asymmetrical OD. The fixed points of the asymmetrical OD can be expressed as $F_{IHSS}(R_1^*, R_1^*, R_1^*, R_2^*)$, where $R_1^* = (\pm x_1^*, \pm y_1^*, \pm x_1^*)$ and $R_2^* = (\pm x_2^*, \pm y_2^*, \pm x_2^*)$, and $x_1^*, x_2^*, y_1^*, y_2^*$ are determined by Eq. (17),

$$\begin{cases} 2\omega x_1^* = y_1^*\left(\sqrt{\epsilon^2 - 4\omega^2 + 4\omega\epsilon Q\dfrac{(2x_1^* + x_2^*)/3}{y_1^*}} - \epsilon\right), \\ 2\omega x_2^* = y_2^*(\sqrt{\epsilon^2 - 4\omega^2 + 4\omega\epsilon Q x_1^*/y_2^*} - \epsilon), \\ 2\epsilon(y_2^*)^2 + Q^2(x_1^*)^2 = \left(1 + \dfrac{\omega Q x_1^*}{y_2^*}\right)\left(\epsilon + \sqrt{\epsilon^2 - 4\omega\left(\omega - \dfrac{\epsilon Q x_1^*}{y_2^*}\right)}\right) + \dfrac{2\omega Q x_1^*}{y_1^*} - 2\omega^2, \\ 2\epsilon(y_1^*)^2 + Q^2((2x_1^* + x_2^*)/3)^2 = \left(1 + \dfrac{\omega Q(2x_1^* + x_2^*)/3}{y_1^*}\right)\left(\epsilon + \sqrt{\epsilon^2 - 4\omega\left(\omega - \dfrac{\epsilon Q(2x_1^* + x_2^*)/3}{y_1^*}\right)}\right) + \dfrac{2\omega Q(2x_1^* + x_2^*)/3)}{y_1^*} - 2\omega^2. \end{cases} \tag{17}$$

NTAD is generated by the TB and coexists with the symmetrical OD and the asymmetrical OD as ω is less than $\omega_{TB} = \frac{\epsilon(1-Q)}{2}$. As the cutoff frequency α decreases to 1, the domains of AD expand while those of the symmetrical OD shrink with the increment of domains of the coexistence of the symmetrical OD and the oscillation state as shown in Fig. 9(b). Moreover, the Hopf bifurcation points is less than the pitchfork bifurcation points (PB1), and the oscillation state is coexisting with the symmetrical OD and the asymmetrical OD. As $Q = 1.2$, there are five domains of different dynamics regimes as AD (area I), oscillation state (area III), NTAD (area IV), and coexistence of symmetrical OD and oscillation state (area V), coexistence of oscillation state and NTAD (area VI) as shown in Figs. 9(c) and 9(d), respectively. The decreasing cutoff frequency α also tends to enlarge AD domains by shrinking the oscillation state domains. There are also asymmetrical OD generated by the pitchfork bifurcation (PB2) as in two coupled oscillators. Note that the oscillation state

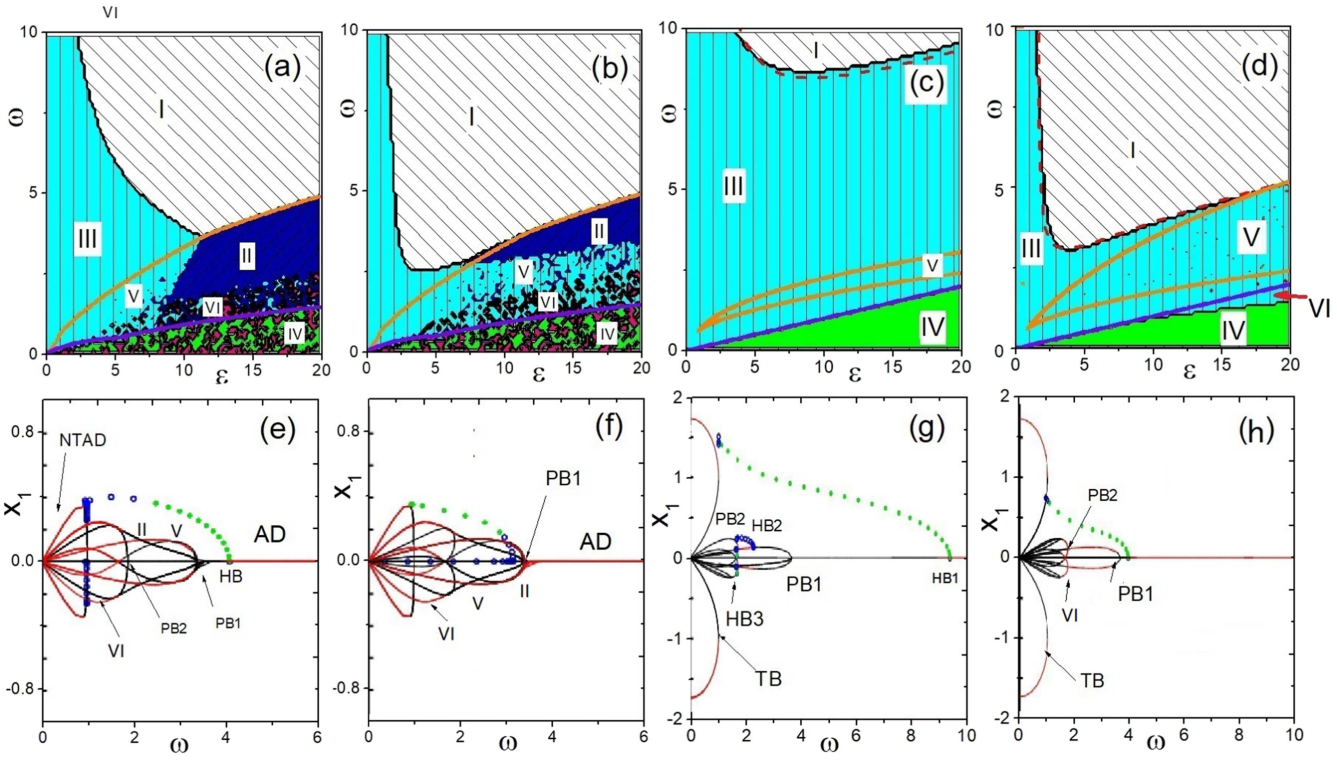

FIG. 9. The phase diagram ω vs ϵ of the globally coupled system with LPF for $N = 4, \alpha = 8, 1$. (a) and (b) $Q = 0.8$, there are six domains as I (AD), II (symmetrical OD), III (oscillation state), IV (coexistence of NTAD symmetrical OD and asymmetrical OD), V (coexistence of oscillation state and symmetrical OD), VI (coexistence of oscillation state, symmetrical OD, and asymmetrical OD), (c) and (d) $Q = 1.2$, there are five domains as I (AD), III (oscillation state), IV (NTAD), V (coexistence of symmetrical OD and oscillation state), and VI (coexistence of NTAD and oscillation state). (e) and (f) The bifurcation diagram of x_1 vs ω for $\epsilon = 10$ with parameters corresponding to (a)–(d) accordingly.

is coexisting with NTAD when ϵ is large, for example, $\alpha = 1, \epsilon = 18$ as shown in area VI in Fig. 9(d).

V. DISCUSSION AND CONCLUSION

We have explored the effects of LPF followed by an active component (amplifiers or attenuators) on the dynamics of diffusively coupled oscillators. Without the LPF, the active component of LPAF tends to enlarge the domain of AD and NTAD, but to shrink that of the symmetrical OD and the oscillation state as it is an attenuator with Q decreasing from 1 to 0. Moreover, the coupled oscillators exhibit rich transition processes from AD to symmetrical OD and then to the coexistence of NTAD and the symmetrical OD. However, if the active component is set to be an amplifier, both AD and symmetrical OD disappear, while the oscillation state and NTAD dominate in the coupled oscillators. The competition between the LPF and the active component plays an important role in the emerging regimes of the coupled oscillators. With the attenuating active component, the stronger filter effects tend to enlarge the AD domain and shrink the symmetrical OD domain by increasing the domain of the coexistence of the symmetrical OD and the oscillation state. In contrast, stronger LPF effects enlarge both the domain of AD and symmetrical OD by stabilizing the formerly unstable HSS and IHSS for the amplifying active component. The effects of the filter here are different from those in time-delay coupled oscillators,[55] where stronger filter effects tend to revoke AD and symmetrical OD. Moreover, our results are realized by filtering signals from the other oscillators; in contrast, the filter in Ref. 58 plays a role of self-filtering effects and may lead to a transition from the homogeneous limit cycle to the inhomogeneous limit cycle.

The LPF influences not only the stability of the fixed points but also the HB point which leads to rich transition processes from AD to symmetrical OD, asymmetrical OD, symmetrical oscillation state, and finally to NTAD due to the amplifying active component. There are two cascades of supercritical pitchfork bifurcations which are corresponding to the AD-symmetrical OD and the symmetrical OD-asymmetrical OD transition. To the best of our knowledge, the cascade transition processes from the symmetrical OD via the asymmetrical OD to symmetrical oscillation state, which is coexisting with a synchronous oscillation state, are new in diffusively coupled oscillators. Note that the bifurcation parameter here is the natural frequency (ω) of the coupled unit, and the final regimes of the coupled oscillators are determined by the local parameter of the coupled unit and the parameter of the LPAF in the coupling term. In contrast, the typical coupling-induced multistability in synthetic genetic networks, e.g., inherent multistability in arrays of autoinducer coupled genetic populations,[65] is determined by the coupling-induced symmetrical break. The symmetrical OD-asymmetrical OD transition was reported as a kind of secondary OD in the parameter space of the coupling strength ϵ of coupled identical oscillators.[63]

Moreover, the NTAD here is originated from a tangential bifurcation which is different with NTAD in Ref. 21, where NTAD is created by a subcritical pitchfork bifurcation in mean-field diffusively coupled oscillators. Since the NTAD is sensitive to the parameter mismatches, the observation of NTAD is subtle in natural and experimental systems as such a parameter mismatch is inevitable in practical coupled oscillators. The coexistence of NTAD and symmetrical OD in coupled oscillators with LPAF followed by an attenuating active component can be controlled to the NTAD state by tuning the active component from attenuation to amplification.

Besides determining the stability of the fixed points, the LPAF also controls the basins of two coexisting states. The stronger filter effects enlarge (or shrink) the basins of symmetrical OD in LPAF with the active component being an amplifier (or attenuator). The existence of different coexisting dynamical regimes in a genetic unit improves the adaptability of the system, since if one of the regimes becomes unprofitable for cell functioning, the genetic unit can easily switch to some of the other coexisting regimes available. Therefore, LPAF is a promising candidate circuit to efficiently control the adaptability of the genetic systems.

This study can be extended to other limit cycles and chaotic oscillators, and we believe that this will improve our understanding of various filter-based diffusively coupled biological and engineering systems.[64] In natural systems, the diffusion of autoinducer molecules between the cell membranes in the genetic regulatory networks is commonly governed by a quorum sensing with a dynamical evolution quite similar to the LPF coupling.[66] The control of AD based on the LPF was recently realized in electrochemical oscillators experimentally.[67] Since the cutoff frequency of the LPAF may change and even eliminate the basins of two coexisting states, the results presented here may be helpful to understand and control the multistability of such coupled systems.

ACKNOWLEDGMENTS

Weiqing Liu is supported by the Natural Science Foundation of China (NSFC) (Grant No. 11765008), the Science and Technology Planning Project of Ganzhou City, and the Qingjiang Program of Jiangxi University of Science and Technology. W.Z. acknowledges support from Research Starting grants from South China Normal University (Grant No. 8S0340) and a project supported by Guangdong Province Universities and Colleges Pearl River Scholar Funded Scheme (2018).

REFERENCES

[1] L. M. Pecora and T. L. Carroll, Phys. Rev. Lett. **64**, 821 (1990).
[2] A. Pikovsky, M. Rosenblum, and J. Kurths, *Synchronization: A Universal Concept in Nonlinear Sciences* (Cambridge University Press, Cambridge, 2001).
[3] A. Koseska, E. Volkov, and J. Kurths, Phys. Rep. **531**, 173 (2013).
[4] A. Koseska, E. Volkov, and J. Kurths, Phys. Rev. Lett. **111**, 024103 (2013).
[5] J. Chen, W. Liu, Y. Zhu, and J. Xiao, Europhys. Lett. **115**(2), 20011 (2016).
[6] M. Y. Kim, R. Roy, J. L. Aron, T. W. Carr, and I. B. Schwartz, Phys. Rev. Lett. **94**, 088101 (2005).
[7] A. Prasad, Y. C. Lai, A. Gavrielides, and V. Kovanis, Phys. Lett. A **318**, 71 (2003).
[8] P. Kumar, A. Prasad, and R. Ghosh, J. Phys. B **41**, 135402 (2008).
[9] G. B. Ermentrout and N. Kopell, SIAM J. Appl. Math. **50**, 125 (1990).
[10] T. Banerjee and D. Biswas, Chaos **23**, 043101 (2013).
[11] Y. Yamaguchi and H. Shimizu, Physica D **11**, 212 (1984).
[12] W. Zou, M. Zhan, and J. Kurths, Phys. Rev. E **98**, 062209 (2018).
[13] S. H. Strogatz, Nature **394**, 316 (1998), Ref. 16.
[14] D. V. RamanaRedy, A. Sen, and G. L. Johnston, Phys. Rev. Lett. **80**, 5109 (1998).
[15] F. M. Atay, Phys. Rev. Lett. **91**, 094101 (2003).
[16] W. Zou, D. V. Senthilkumar, A. Koseska, and J. Kurths, Phys. Rev. E **88**, 050901(R) (2013).
[17] K. Konishi, Phys. Rev. E **68**, 067202 (2003).

[18]R. Karnatak, R. Ramaswamy, and A. Prasad, Phys. Rev. E **76**, 035201(R) (2007).
[19]A. Sharma and M. D. Shrimali, Phys. Rev. E **85**, 057204 (2012).
[20]T. Banerjee and D. Ghosh, Phys. Rev. E **89**, 062902 (2014).
[21]T. Banerjee and D. Ghosh, Phys. Rev. E **89**, 052912 (2014).
[22]A. Sharma, P. R. Sharma, and M. D. Shrimali, Phys. Lett. A **376**, 1562 (2012).
[23]N. K. Kamal, P. R. Sharma, and M. D. Shrimali, Phys. Rev. E **92**, 022928 (2015).
[24]V. Resmi, G. Ambika, and R. E. Amritkar, Phys. Rev. E **84**, 046212 (2011).
[25]Y. Goto and K. Kaneko, Phys. Rev. E **88**, 032718 (2013).
[26]N. Suzuki, C. Furusawa, and K. Kaneko, PLoS One **6**, e27232 (2011).
[27]A. Koseska, E. Ullner, E. Volkov, J. Kurths, and J. G. Ojalvo, J. Theor. Biol. **263**, 189 (2010).
[28]E. Ullner, A. Koseska, J. Kurths, E. Volkov, H. Kantz, and J. Garca-Ojalvo, Phys. Rev. E **78**, 031904 (2008).
[29]E. Ullner, A. Zaikin, E. I. Volkov, and J. Garcia-Ojalvo, Phys. Rev. Lett. **99**, 148103 (2007).
[30]A. Koseska, E. Volkov, and J. Kurths, Europhys. Lett. **85**, 28002 (2009).
[31]R. Curtu, Physica D **239**, 504 (2010).
[32]K. P. Zeyer, M. Mangold, and E. D. Gilles, J. Phys. Chem. **105**, 7216 (2001).
[33]B. K. Bera, C. Hens, S. K. Bhowmick, P. Pal, and D. Ghosh, Phys. Lett. A **380**(1), 130–134 (2016).
[34]C. R. Hens, O. I. Olusola, P. Pal, and S. K. Dana, Phys. Rev. E **88**, 034902 (2013).
[35]W. Liu, G. Xiao, Y. Zhu, M. Zhan, J. Xiao, and J. Kürths, Phys. Rev. E **91**, 052902 (2015).
[36]S. S. Chaurasia, M. Yadav, and S. Sinha, Phys. Rev. E **98**, 032223 (2018).
[37]J. Yang, Phys. Rev. E **76**, 016204 (2007).
[38]W. Liu, J. Xiao, L. Li, Y. Wu, and M. Lu, Nonlinear Dyn. **69**, 1041 (2012).
[39]G. B. Ermentrout, Physica D **41**, 219 (1990).
[40]Z. Hou and H. Xin, Phys. Rev. E **68**, 055103 (2003).
[41]H. Bi, X. Hu, X. Zhang, Y. Zou, Z. Liu, and S. Guan, Europhys. Lett. **108**, 50003 (2014).
[42]W. Liu, X. Wang, S. Guan, and C. H. Lai, New J. Phys. **11**, 093016 (2009).
[43]K. Ponrasu, K. Sathiyadevi, V. K. Chandrasekar, and M. Lakshmanan, Europhys. Lett. **124**, 20007 (2018).
[44]C. R. Hens, P. Pal, S. K. Bhowmick, P. K. Roy, A. Sen, and S. K. Dana, Phys. Rev. E **89**, 032901 (2014).
[45]T. Knapen, J. Brasscamp, J. Pearson, R. van Ee, and R. Blake, J. Neurosci. **31**, 10293 (2011).
[46]E. Ozbudak, M. Thattai, H. Lim, B. Shraiman, and A. van Oudenaarden, Nature **427**, 737 (2004).
[47]J. J. Tyson, K. Chen, and B. Novak, Nat. Rev. Mol. Cell Biol. **2**, 908 (2001).
[48]T. Banerjee and D. Ghosh, Phys. Rev. E **89**, 052912 (2014).
[49]D. Ghosh and T. Banerjee, Phys. Rev. E **90**, 062908 (2014).
[50]A. M. Nakashima, M. J. Borland, and S. M. Abel, Ind. Health **45**, 318 (2007).
[51]L. Stark, *Neurological Control Systems: Studies in Bioengineering* (Plenum Press, New York, 1968).
[52]K. Pyragas, V. Pyragas, I. Z. Kiss, and J. L. Hudson, Phys. Rev. Lett. **89**, 244103 (2002).
[53]H. Ma, F. Min, and Y. Wang, Chin. J. Phys. **56**(5), 2488–2499 (2018).
[54]G. F. Keyser, J. A. Holloway, and D. D. Prather, J. Interdiscipl. Cycle Res. **10**, 239 (1979).
[55]W. Zou, M. Zhan, and J. Kurths, Phys. Rev. E **95**, 062206 (2017).
[56]M. Y. Kim, C. Sramek, A. Uchida, and R. Roy, Phys. Rev. E **74**, 016211 (2006).
[57]M. C. Soriano, F. Ruiz-Oliveras, P. Colet, and C. R. Mirasso, Phys. Rev. E **78**, 046218 (2008).
[58]T. Banerjee, D. Biswas, D. Ghosh, B. Bandyopadhyay, and J. Kurths, Phys. Rev. E **97**, 042218 (2018).
[59]D. Lancaster, *Active-Filter Cookbook* (Howard W. Sams and Co., 1975), pp. 8–10, ISBN: 0-672-21168-8.
[60]W. M. Liu, J. Math. Anal. Appl. **182**, 250 (1994).
[61]G. Xiao, W. Liu, Y. Lan, and J. Xiao, Nonlinear Dyn. **93**, 1047 (2018).
[62]A. Sharma and M. D. Shrimali, Phys. Rev. E **85**, 057204 (2012).
[63]A. Zakharova, I. Schneider, Y. N. Kyrychko, K. B. Blyuss, A. Koseska, B. Fiedler, and E. Scholl, Europhys. Lett. **104**, 50004 (2013).
[64]A. Schenck zu Schweinsberg and U. Dressler, Phys. Rev. E **63**, 056210 (2001).
[65]A. Koseska, E. Volkov, A. Zaikin, and J. Kurths, Phys. Rev. E **75**, 031916 (2007).
[66]A. Kuznetsov, M. Kærn, and N. Kopell, SIAM J. Appl. Math. **65**, 392 (2004).
[67]W. Zou, J. L. Ocampo-Espindola, D. V. Senthilkumar, I. Z. Kiss, M. Zhan, and J. Kurths, Phys. Rev. E **99**, 032214 (2019).